Applied Thermal Engineering 50 (2013) 422–428

Contents lists available at SciVerse ScienceDirect

Applied Thermal Engineering

journal homepage: www.elsevier.com/locate/apthermeng

The application and experimental validation of a heat and mass transfer analogy model for the prediction of mass transfer in solar distillation systems

P.T. Tsilingiris

Department of Energy Engineering, Heat Transfer Laboratory, Technological Education Institution of Athens, A. Spyridonos Street, GR 122 10 Egaleo, Athens, Greece

HIGHLIGHTS

- Modeling of heat and mass transfer in solar distillation systems.
- Application of Chilton–Colburn model for modeling mass transfer.
- Model assessment through field experimental measurements.
- Validation of analysis at a wide range of operating conditions.

ARTICLE INFO

Article history:
Received 2 March 2012
Accepted 3 July 2012
Available online 14 July 2012

Keywords:
Solar distillation systems
Mass transfer modeling
Chilton–Colburn analogy
Water vapor diffusion
Yield outflow prediction

ABSTRACT

In the present investigation efforts have been made for the validation of a new theoretical model, allowing the prediction of mass transport in the barometric enclosure of solar distillation systems. It appears that this model which is based on the Chilton–Colburn analogy being applicable for a broad range of Prandtl and Schmidt dimensionless numbers, can potentially be employed at a wide range of operating conditions and may turn out to become an accurate, more universal alternative to the widely known Dunkle's theoretical model. The comparative validation is carried out employing a set of field experimental measurements which were derived in a passive solar still under favorable climatic conditions during mid summer, aiming validation at higher operating temperature conditions. It is derived that the model is impressively accurate for predictions of the derived measurements in a wide range of average operating temperatures higher than about 70 °C and up to about 0.2 gr/m^2 s yields.

1. Introduction

Parallel to the substantial earlier research activities and the successful enormous demonstration work programme that has been developed during the last several decades in various geographical regions of the world and to the first steps toward the commercialization of solar distillation systems [1], a substantial ongoing research activity on various aspects of these systems is still carried out worldwide. This contributes toward the deeper understanding of the physical processes involved, as well as improving our level of knowledge on certain interesting scientific aspects of this technology, like the combined heat transfer and mass transport processes, which still appears to be far of being complete. It is surprising that the most influential theory on transport processes in these systems was developed five decades ago by Dunkle [2] and apart from certain controversies and objections which have occasionally been reported in the literature [3–7], it still enjoys the confidence of the worldwide scientific community when it is properly applied under the specific limitations according to which it was initially developed as reported by Malik et al. [8] and Adhikari et al. [9]. The limitations of this theory are mainly associated with the upper operational temperature level, beyond which dry air thermophysical properties assumption is violated and the enclosure shape restrictions, which are imposed by the parallel or small inclination plane enclosure geometry. Both these factors affect the convective heat transfer conditions and the evaluation of the relevant heat transfer coefficient as it was reported by Porta-Gandara et al [10], Rubio et al. [11] and Tiwari and Tripathy [12], which strongly determines the mass transport and outflow of distillate. Although most systems involve simple cavity geometries for which this theory is valid with a sufficient accuracy, investigations have been carried out, and procedures have been recommended for application in situations when the original cavity geometry assumption is not valid, by Kumar and Tiwari [13] and Djebedjian and Rayan [14]. Apart of this theory an alternative mass

E-mail address: ptsiling@teiath.gr.

1359-4311/$ – see front matter © 2012 Elsevier Ltd. All rights reserved.
http://dx.doi.org/10.1016/j.applthermaleng.2012.07.007

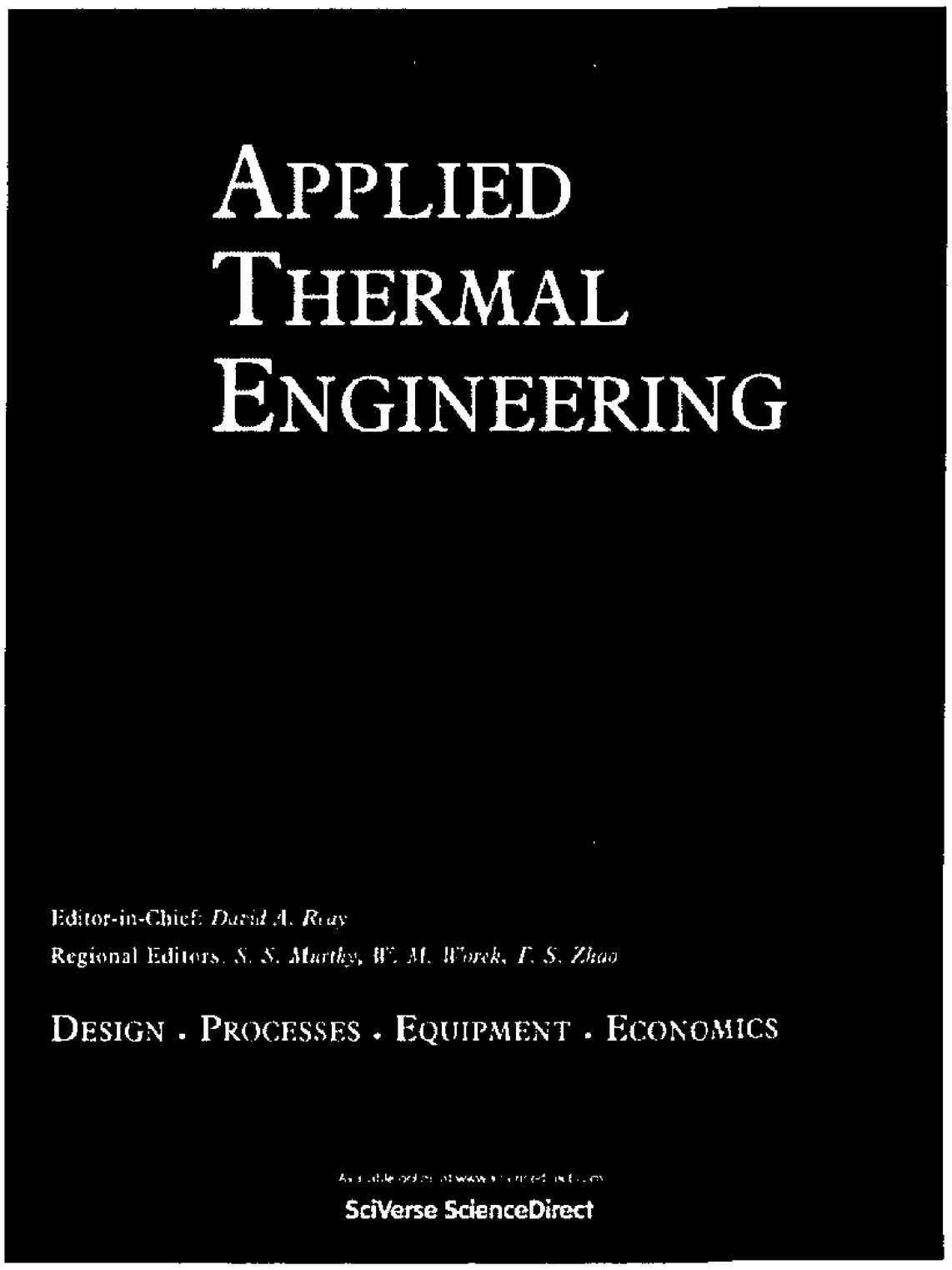

(This is a sample cover image for this issue. The actual cover is not yet available at this time.)

transfer model based on Chilton–Colburn analogy principles has been recently recommended by Tsilingiris [7], for application in a wide range of operating conditions.

The aim of the present investigation is the application of this model for the prediction of the mass transfer rates in properly thermally insulated solar stills operating in the field under meteorological conditions corresponding to a hot and dry Mediterranean mid summer climate. The derived results from these experimental measurements which it is believed that have been carried out under the higher typically obtainable operating temperatures using shallow basin passive solar stills of ordinary design, were employed for the partial comparative validation of the proposed model, at least as far as the available field measurements is concerned.

2. The analysis and application of the Chilton–Colburn analogy model

Solar distillation systems are basically simple devices consisting generally in principle of a saline water and air interface inside a barometric top glazed confined space, in which a complete evaporation and condensation cycle occurs. With the exception of the wetted wick type based solar still design, most systems comprise of a saline water layer that is contained in a basin at the bottom of a barometric enclosure with a free horizontal air and water interface. This shallow water body is heated by the absorption of the incident solar radiation, which is transmitted through the top glazing system causing continuous evaporation of water from its free liquid surface. Owing to the temperature difference between the water surface and the top glazing system, convective circulation occurs which is responsible for the fluid flow, condensation of the water vapor at the top glazing surface, and outflow of distillate. The given enclosure geometry determines the internal flow structures which may become very complex for high sloped triangular and trapezoid cavity shapes, since the particular geometry affects considerably the convective heat transfer and mass transport phenomena. However, the thermal convection in a simple horizontal fluid layer under the effect of a destabilizing temperature gradient, which is the case when the top condensing surface is nearly parallel to the horizontal liquid surface something that occurs very often in practice as also occurred during the course of the developed measurements, has been reported extensively earlier in the literature by many investigators like Jacob [15], McAdams [16] and Hollands [17,18]. For conditions corresponding to strong turbulence the following correlation has been derived,

$$Nu = \frac{h_{cv}\cdot L}{k} = 0.075\cdot(Gr\cdot Pr)^{1/3} = 0.075\cdot Ra^{1/3} \tag{1}$$

which is valid according to McAdams [16], for $3.2\times10^5 < Gr < 10^7$. As the turbulence level increases substantially the heat transfer, it also enhances considerably the mass transport owing to the combined phenomena of mass diffusion and bulk fluid motion, by removing higher concentration mixture away from the surface and replacing it by lower concentration from above. In any case, heat and mass transfer phenomena in the confined space of solar distillation systems occur through two diffusive boundary layers confined at the free open liquid and the top condensing surfaces, which are separated by a well mixed layer of uniform temperature and concentration, something that has been confirmed extensively by numerous earlier investigations like those by Baum [19] and Hollands [17]. Water vapor pressure differentials caused by the low temperature condensing plate causes diffusion of vapor upwards, the mass flow being sustained by continuous evaporation from the liquid interface. Earlier investigations by Sharpley and Boetler [20] have indicated that owing to the different molar masses of air and water vapor, as well as composition of the two mixture components at the water and glazing temperatures, the driving force for the convective circulation is not the ordinary temperature difference $\Delta T = T_w - T_g$ as occurs in the usual thermal systems but the equivalent temperature difference,

$$\Delta T^* = \Delta T + \frac{[P(t_w) - P(t_g)]\cdot(M_a - M_w)\cdot T_w}{M_a\cdot P_0 - P(t_w)\cdot(M_a - M_w)} \tag{2}$$

This was first employed by Dunkle [2], to develop the following simple expression for modeling of the convective heat transfer coefficient in solar stills, based on the correlation (1) as well as assuming operation conditions corresponding to lower than about 50 C at which thermophysical properties of the saturated vapor mixture differ slightly from those corresponding to dry air,

$$h_{cv} = 0.884\cdot\left[t_w - t_g + \frac{[P(t_w) - P(t_g)]\cdot T_w}{268.9 - P(t_w)}\right]^{1/3} \tag{3}$$

In the previous expressions the functional dependence of the saturated vapor pressure with temperature was derived by fitting data from standard international tables for steam with the following polynomial expression,

$$P(t) = A_0 + A_1\cdot t + A_2\cdot t^2 + A_3\cdot t^3 + A_4\cdot t^4 \tag{4}$$

with the values of numerical constants given in Table 1.

Aiming at expanding the validity range of the previous convective heat transfer coefficient expression for application at a broad range of higher operating conditions at which the correlation (1) is valid, the thermophysical properties of saturated vapor mixture were derived independently from simple linear mixing procedures and molecular considerations by Tsilingiris [21,22], and the results were found in very good agreement, as well as in good agreement with a limited number of earlier measurements in the literature. According to these analyses it was found that the convective heat transfer coefficient can be evaluated by the following expression,

Table 1
Values of numerical constants in the fit expressions (10) to (16) allowing the evaluation of saturated mixture thermophysical properties (adapted from references [7,21,22]).

Physical quantity	Units	Values of numerical constants
P_w	kPa	$A_0 = 1.131439334$, $A_1 = -3.750393331\times10^{-2}$, $A_2 = 5.591559189\times10^{-3}$, $A_3 = -6.220459433\times10^{-5}$, $A_4 = 1.10581611\times10^{-6}$
ρ_m	Kg/m^3	$B_0 = 1.299995662$, $B_1 = -6.043625845\times10^{-3}$, $B_2 = 4.697926602\times10^{-5}$, $B_3 = -5.760867827\times10^{-7}$
μ_m	Kg/m s	$C_0 = 1.685731754\times10^{-5}$, $C_1 = 9.151853945\times10^{-8}$, $C_2 = -2.16276222\times10^{-9}$, $C_3 = 3.413922553\times10^{-11}$, $C_4 = -2.644372665\times10^{-13}$
k_m	w/m K	$K_0 = 0.02416826077$, $K_1 = 5.526004579\times10^{-5}$, $K_2 = 4.631207189\times10^{-7}$, $K_3 = -9.489325324\times10^{-9}$
α_m	m^2/s	$E_0 = 1.881493006\times10^{-5}$, $E_1 = 8.027692454\times10^{-8}$, $E_2 = 1.496456991\times10^{-9}$, $E_3 = -2.112432387\times10^{-11}$
$D_{w,a}$	m^2/s	$Q_0 = 1.820034881\times10^{-5}$, $Q_1 = 1.324098731\times10^{-7}$ and $Q_2 = 1.978458093\times10^{-10}$
c_{pm}	kJ/kg K	$F_0 = 1.088022802$, $F_1 = -0.01057758092$, $F_2 = 4.769110559\times10^{-4}$, $F_3 = -7.898561559\times10^{-6}$ and $F_4 = 5.122303796\times10^{-8}$
Pr	(−)	$N_0 = 0.7215798365$, $N_1 = -3.703124976\times10^{-4}$, $N_2 = 2.240599044\times10^{-5}$, $N_3 = -4.162785412\times10^{-7}$, $N_4 = 4.969218948\times10^{-9}$

$$h_{cv} = 0.075 \cdot k_m \cdot \left(\frac{g \cdot \rho_m \cdot \beta}{\mu_m \cdot \alpha_m}\right)^{1/3} \cdot \left[(t_w - t_g) + \frac{T_w \cdot [P(t_w) - P(t_g)] \cdot (M_a - M_w)}{M_a \cdot P_o - P(t_w) \cdot (M_a - M_w)}\right]^{1/3} \quad (5)$$

with the average values of saturated mixture thermophysical properties k_m, ρ_m, μ_m and α_m being evaluated at the average still temperature, $\bar{t} = (t_w + t_g)/2$.

Based on mass balance considerations and the derived expressions (3) and (5) for the evaluation of the convective heat transfer coefficient, Dunkle has developed the following expression for the prediction of the mass flow of yield,

$$\dot{m}_w = \frac{h_{cv}}{c_{pa}} \cdot \frac{R_a}{R_w} \cdot \frac{P_o \cdot [P(t_w) - P(t_g)]}{[(P_o - P(t_w))] \cdot [(P_o - P(t_g))]} \quad (6)$$

which can be simplified significantly under the assumption of negligible saturation pressures, $P(t_w) << P_o$ and $P(t_g) << P_o$, something which is basically valid at lower operating temperatures.

However, owing to the inefficiency of the previously developed model to predict measurements at a wide range of operational conditions, alternative analyses based on the Chilton–Colburn analogy approach have been earlier attempted by Shawaqfeh and Farid [23], Hongfei et al. [24] and Tsilingiris [7]. Chilton–Colburn analogy, which is an extension of the Reynolds analogy between momentum heat and mass transfer at a wider range of Prandtl and Schmidt numbers predicts according to Coulson and Richardson [25] identical values of the heat and mass j numbers. It has been demonstrated by Chilton and Colburn [26] that,

$$\frac{St}{St_{ms}} = \left(\frac{Sc}{Pr}\right)^{2/3} \quad (7)$$

with St and St_{ms} the Stanton and Stanton mass dimensionless numbers respectively, which is valid for $0.6 < Pr < 60$ and $0.6 < Sc < 3000$. According to this as it was recently reported by Tsilingiris [7], the mass outflow of distillate can be evaluated irrespectively of the average still temperature level by the following expression,

$$\frac{\dot{m}_w}{h_{cv}} = \frac{1}{\rho_m \cdot c_{pm}} \cdot \frac{P_o}{P_{LM}} \cdot \frac{1}{R_w} \cdot \left[\frac{P(t_w)}{T_w} - \frac{P(t_g)}{T_g}\right] \cdot Le^{-2/3} \quad (8)$$

The product $(\rho \cdot c_p)_m$ in the previous expression corresponds to average saturated mixture properties and P_{LM} represents the logarithmic mean pressure in Pa which is given by the following expression,

$$P_{LM} = \frac{[P_o - P(t_w)] - [P_o - P(t_g)]}{\ln \frac{P_o - P(t_w)}{P_o - P(t_g)}} \quad (9)$$

The Lewis number is calculated as,

$$Le = \frac{\alpha_m}{D_{w,a}(\bar{t})} \quad (10)$$

where $D_{w,a}$ is the diffusion coefficient of water vapor into air. A literature review has shown several theoretical and semi-empirical models for the evaluation of the temperature depended diffusion coefficient of water vapor to air in the temperature range of interest. A comparative presentation of calculated results has shown a sufficient agreement between earlier and more recently proposed models, while indicating a significant up to about 80% increase of their initial value for a corresponding temperature increase between 0 and 100 °C [7]. For the purpose of the present investigation, the diffusion coefficient was calculated according to the Chapman-Enskog model, taken as typical.

The values of all saturated vapor mixture thermophysical properties except the diffusion coefficient and Prandtl number were calculated according to [21], by the following polynomial fit expressions,

$$\rho_m = B_0 + B_1 \cdot t + B_2 \cdot t^2 + B_3 \cdot t^3 \quad (11)$$

$$\mu_m = C_0 + C_1 \cdot t + C_2 \cdot t^2 + C_3 \cdot t^3 + C_4 \cdot t^4 \quad (12)$$

$$k_m = K_0 + K_1 \cdot t + K_2 \cdot t^2 + K_3 \cdot t^3 \quad (13)$$

$$\alpha_m = E_0 + E_1 \cdot t + E_2 \cdot t^2 + E_3 \cdot t^3 \quad (14)$$

$$c_{pm} = F_0 + F_1 \cdot t + F_2 \cdot t^2 + F_3 \cdot t^3 + F_4 \cdot t^4 \quad (15)$$

while the values for the Prandtl number and the diffusion coefficient were calculated as derived by Tsilingiris from [22] and [7] respectively, by the following expressions,

$$Pr_m = N_0 + N_1 \cdot t + N_2 \cdot t^2 + N_3 \cdot t^3 + N_4 \cdot t^4 \quad (16)$$

$$D_{w,a}(t) = Q_0 + Q_1 \cdot t + Q_2 \cdot t^2 \quad (17)$$

with the indicated values of numerical constants as shown in Table 1.

3. The experimental measurements

Extensive measured data were derived during a recent field experimental investigation in a single slope passive solar still of ordinary design, the results of which have been recently discussed in greater detail by Tsilingiris [27]. Therefore a brief description of the experimental device and measurement system will be reported here.

The experimental solar still of a collapsible design, as it is schematically shown in Fig. 1, was made of a brass sheet frame 2.5 mm thick and a detachable 3 mm aluminum sheet pool tray with dimensions 0.50 × 0.70 m, painted with a matt black paint over a suitable primer. The frame was glazed at the top using an ordinary glass cover at 15° inclination angle, facing south, which was properly secured at the top lips of the metal sheet frame using screw clamps and rubber gaskets pasted with a silicone grease component for protection against infiltration of water vapor and for adequate mechanical rigidity against strong blowing winds. Efforts have been made for the proper thermal insulation of the experimental device using rigid layers of polymer thermal insulation material 3 and 5 cm thick over the opaque peripheral walls and bottom of the experimental unit respectively.

Thin wired, calibrated K type thermocouples were employed for temperature recording the average brine and top glazing average temperature. For the glazing surface measurements, the thermocouple junctions were carefully glued under pressure with an appropriate length of thermocouple wire running parallel to the glazing surface for minimizing conduction heat loss errors. A number of thermocouples were attached at various locations over the top and the lower surface of the glazing during the course of exploratory tests. The glazing surface temperature was recorded by the underside thermocouple junction, which was effectively shaded by the quantity of the opaque bonding adhesive material spread over the opposite, ambient side exposed junction. Ambient temperature

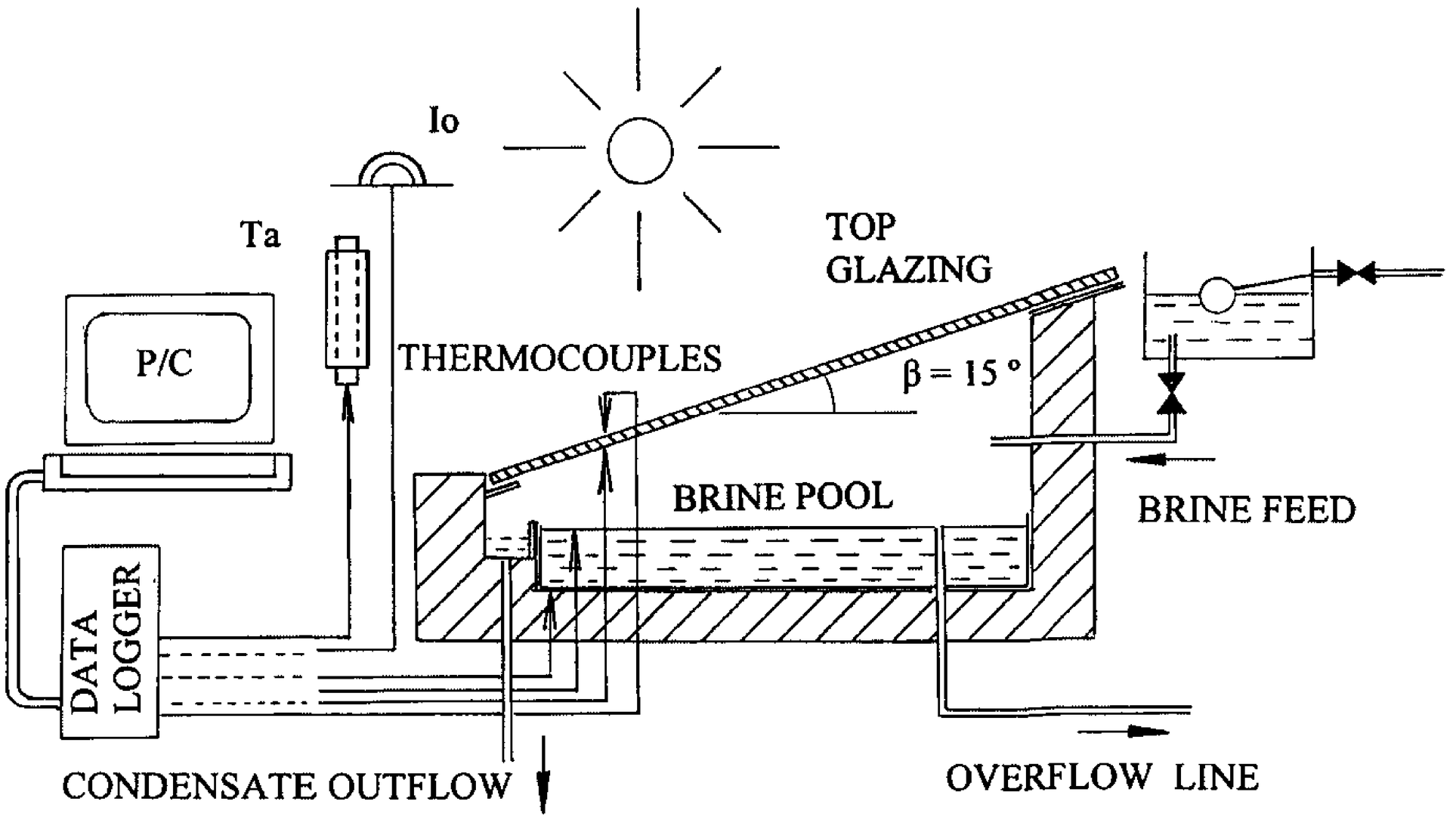

Fig. 1. The simplified schematic of the employed experimental solar still with the monitoring system, various sensors and the data acquisition equipment.

was recorded using a naturally ventilated, properly shielded K type thermocouple while total solar radiation measurements at the horizontal surface of the pool tray were derived by using a Kipp and Zonnen CM10 pyranometer. The measurement of volumetric outflow of distillate was recorded in 15 min intervals, using graduated jars with a least count of 1 ml volumes, allowing mass evaluation accuracy as high as 2% for operation during time periods of higher yields which was strongly degraded for sampling periods of very low yield. All thermocouples and analog output signals were connected through a data acquisition system, based on the use of a TC-08 data logger with a conventional microcomputer. The data logger which ensures basic temperature accuracy of ±0.2% and ±0.5 °C and typically ±0.2% of reading and ±10 μV voltage accuracy, was programmed to scan all sensors typically at 1 min time intervals.

The measurements have been carried out during the course of several experimental runs under hot dry and windy summer conditions in Athens, 38 N latitude, being a typical summer climate for the Mediterranean region. Indicative results corresponding to a specific daily run are shown in Fig. 2, in which the variation of incident solar radiation and ambient temperature (I_o) and (t_a) are shown, along with the brine and glazing temperatures t_w and t_g respectively. In the same plot the distillate yield measured data m_{me} during the daily period of derived measurements were plotted with small circle data points connected by a solid line. Corresponding predictions m_p in (gr/m^2 s) that have been derived according to the present analysis using the Chilton–Colburn analogy model have also comparably been plotted with a solid line in the same figure, showing a very good agreement with measurements.

During the course of measurements, although maximum brine temperatures as high as 76 °C were recorded, which is believed to represent the highest typically obtainable brine temperatures with ordinary shallow basin passive solar distillers under the specified weather conditions, the calculated maximum recorded average still temperature scarcely exceeded 70 °C, with temperature differences typically between 5 and 10 °C.

Under these conditions, although the measured yields were found varying within a relatively narrow range between about 0.003 to 0.2 gr/m^2 s, less than about 5% of the measurements were found corresponding to $Ra^* \leq 10^6$. These limited measurements representing mainly very low yields, were ignored having been considered as of a lower accuracy and reliability owing to the respective lower Ra* numbers for which the correlation (2), valid for conditions of strong turbulence may not be valid with a sufficient accuracy, as well as due to the degraded mass measurement accuracy level at very low yields.

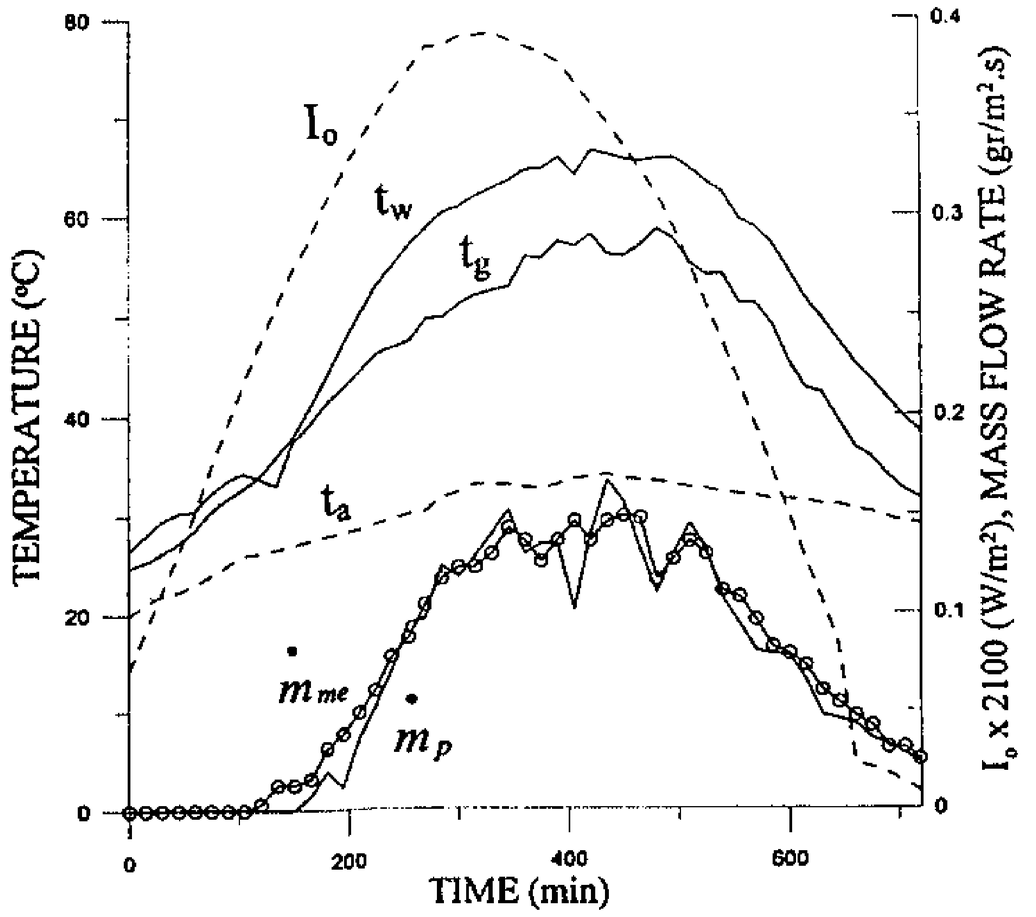

Fig. 2. Typical experimental results for a specific daily run showing the incident solar radiation at the horizontal plane and ambient temperature, I_o and t_a respectively, along with brine t_w and glazing t_g temperatures. In the same plot the measured and predicted yields m_{me} and m_p respectively, are also comparatively shown.

4. Results and discussion

The predicted mass flow rate depends strongly according to the expression (8) on the accurate evaluation of the convective heat transfer coefficient. Comparative values of this strongly influential parameter as derived from the simple and more precise models (3) and (5) respectively were calculated for $\Delta T = 5$, 10 and 15 °C at the entire range of average still temperatures varying between 30 and 100 °C. The derived results from both models were plotted in Fig. 3, showing a significant increase of h_{cv} as ΔT increases from 5 to 15 °C for a fixed value of t_w. It is also shown that for a fixed ΔT although close values are derived from both models at lower than about $t_w = 60$ °C, the derived convective heat transfer coefficient from the simplified model is getting comparably higher as the temperature increases up to about $t_w = 100$ °C.

The derived measurements were further employed for direct comparisons with predictions according to the developed theoretical model. For each measurement the temperatures t_w and t_g were employed for the calculation of the corresponding pertinent thermophysical properties from expressions (11) to (17) and the evaluation of the convective heat transfer coefficients according to simplified and the more accurate expressions (3) and (5) respectively. Based on these values the corresponding predicted yield was calculated through the respective expressions (8) to (10).

4.1. The experimental validation of theoretical predictions

The derived results corresponding to the calculations based on the approximate expression (3) for the evaluation of the convective heat transfer coefficient are shown in Fig. 4 in which the mass outflow measurements from runs 1 to 7 were plotted against theoretical predictions. As derived from the distribution of data points within the unity slope diagonal line, there is a fairly good agreement between derived predictions and measurements in the whole range of measured yield, although a slight overprediction begins to develop at higher than about 0.1 gr/m^2 s yields,

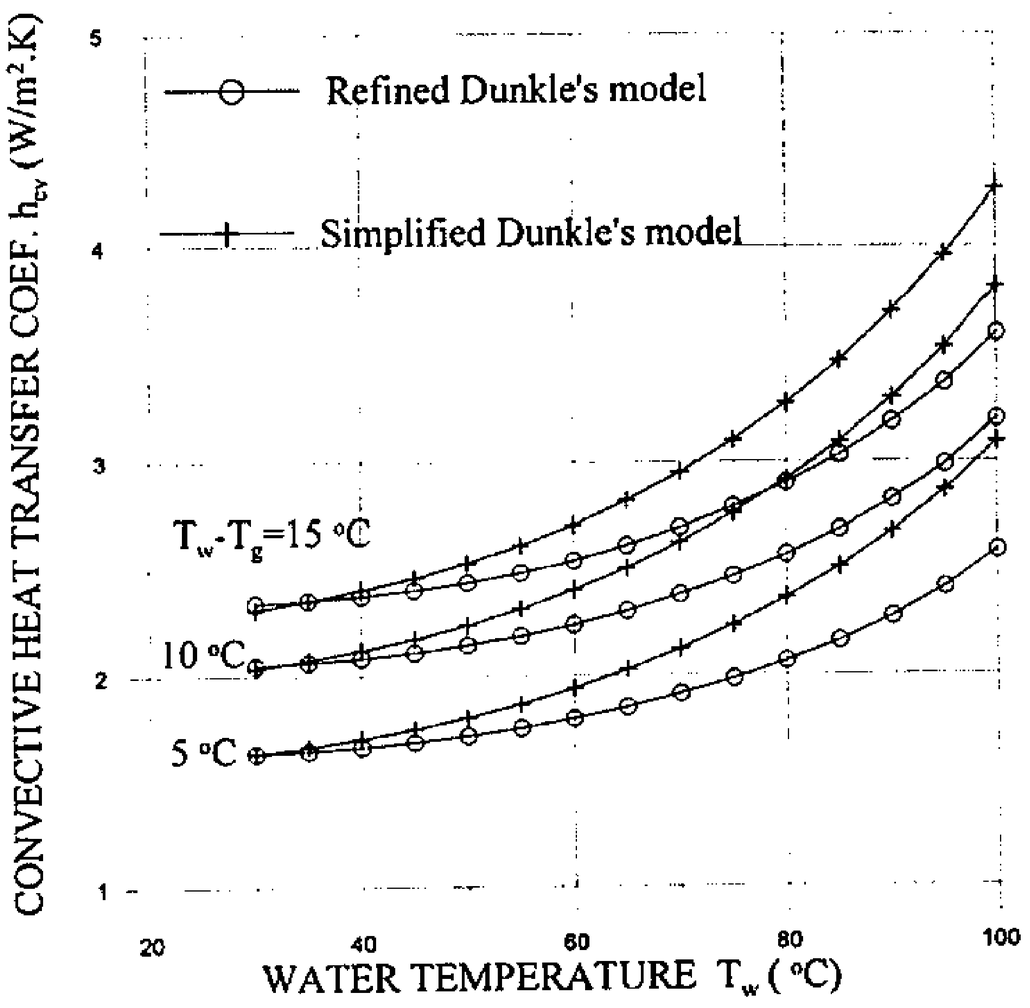

Fig. 3. The dependence of the convective heat transfer coefficient as a function of the brine temperature for typical values of $\Delta T = T_w - T_g$ of 5, 10 and 15 °C according to the simplified expression (3) and the refined model (5).

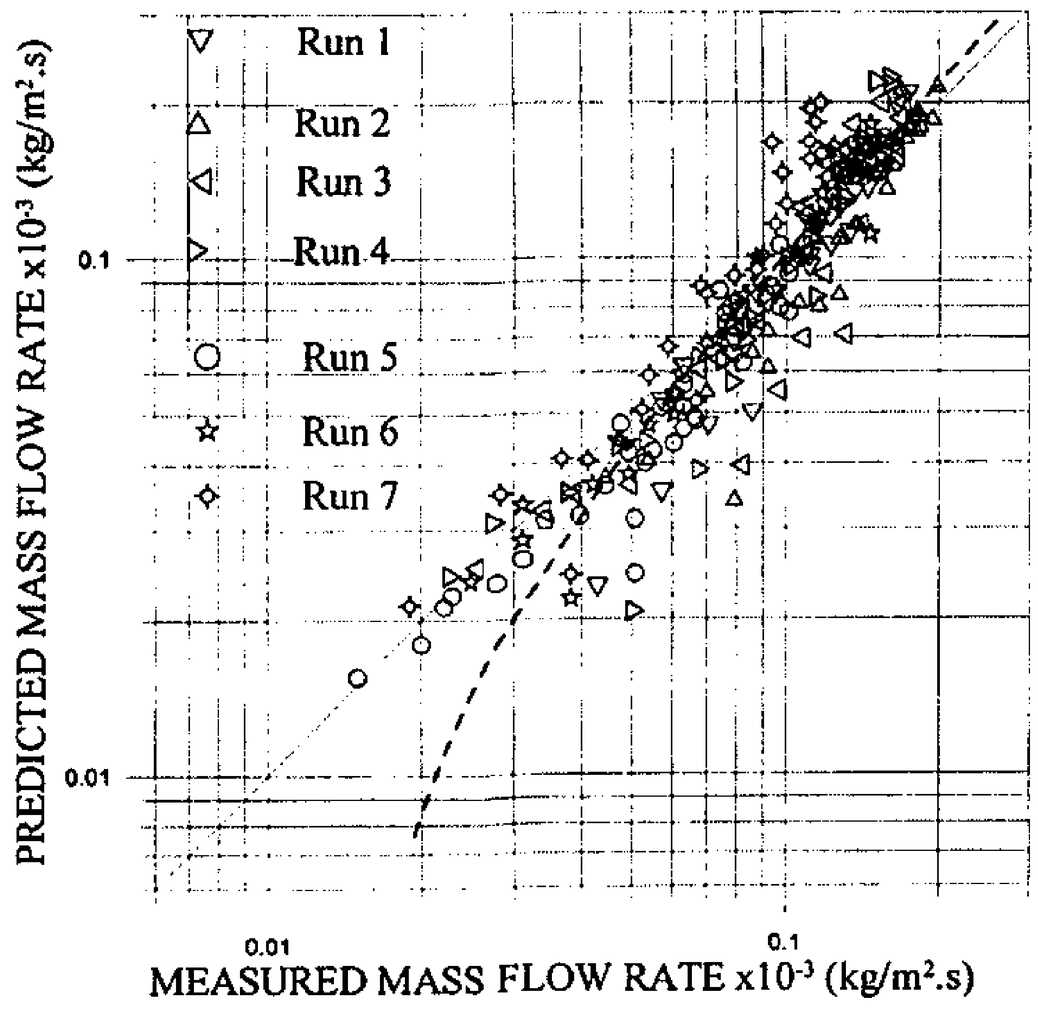

Fig. 4. Yield predictions according to the theoretical model against derived field measurements according to convective heat transfer coefficient values as derived from the simplified expression (3), with the best fit line expression (17) shown in dashed line within the plotted discrete data points.

corresponding to respective higher temperatures at which a substantial fraction of the whole sample of data is distributed. This is shown by the best fit regression line, which is represented by the following expression with the corresponding coefficient of determination (COD),

$$\dot{m}_p = \lambda_1 \cdot \dot{m}_{me} - \lambda_2, \quad \mathrm{COD} = 0.8511 \tag{18}$$

where $\lambda_1 = 1.654$ and $\lambda_2 = 0.0148$ kg/m^2 s.

This expression which was plotted with a dashed line in the same figure, clearly indicates that the higher deviation between predictions and measurements shifts the fit line to a slightly higher than unity slope.

The corresponding results derived by the same model using the more accurate expression (5) for the convective heat transfer coefficient were plotted in Fig. 5, in which measurements were also plotted against predictions for the data of all runs. A very good agreement is shown between predictions and measurements as indicated by the close distribution of data points within the unity slope line. This is also confirmed by the following linear fit regression expression,

$$\dot{m}_p = \xi_1 \cdot \dot{m}_{me} - \xi_2, \quad \mathrm{COD} = 0.8459 \tag{19}$$

where $\xi_1 = 1.0396$ and $\xi_2 = 0.0098$ kg/m^2 s. This expression was plotted with dashed line and almost coincides with the unity slope line, underlining the significant effect of accurate evaluation of the convective heat transfer coefficient by the expression (5).

4.2. Prediction of the temperature dependence of measurements. The influence of temperature level

A statistical review of the complete set of derived measurements from all runs has indicated that about 75% of the data correspond to the temperature difference range between $5 < \Delta T < 10$ °C. At the same time an appreciably lower fraction of

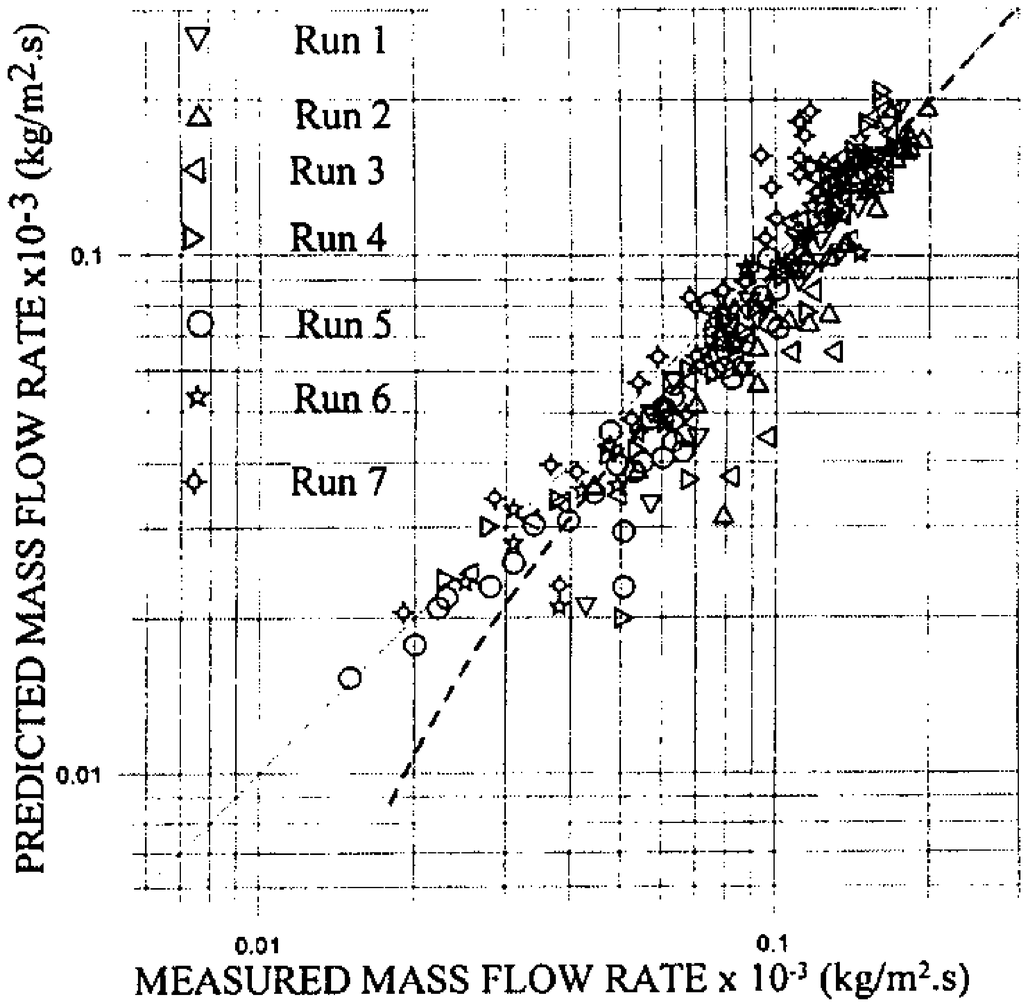

Fig. 5. Yield predictions according to the theoretical model against derived field measurements according to convective heat transfer coefficient values as derived from the refined expression (4), with the best fit line expression (18) shown in dashed line within the plotted discrete data points.

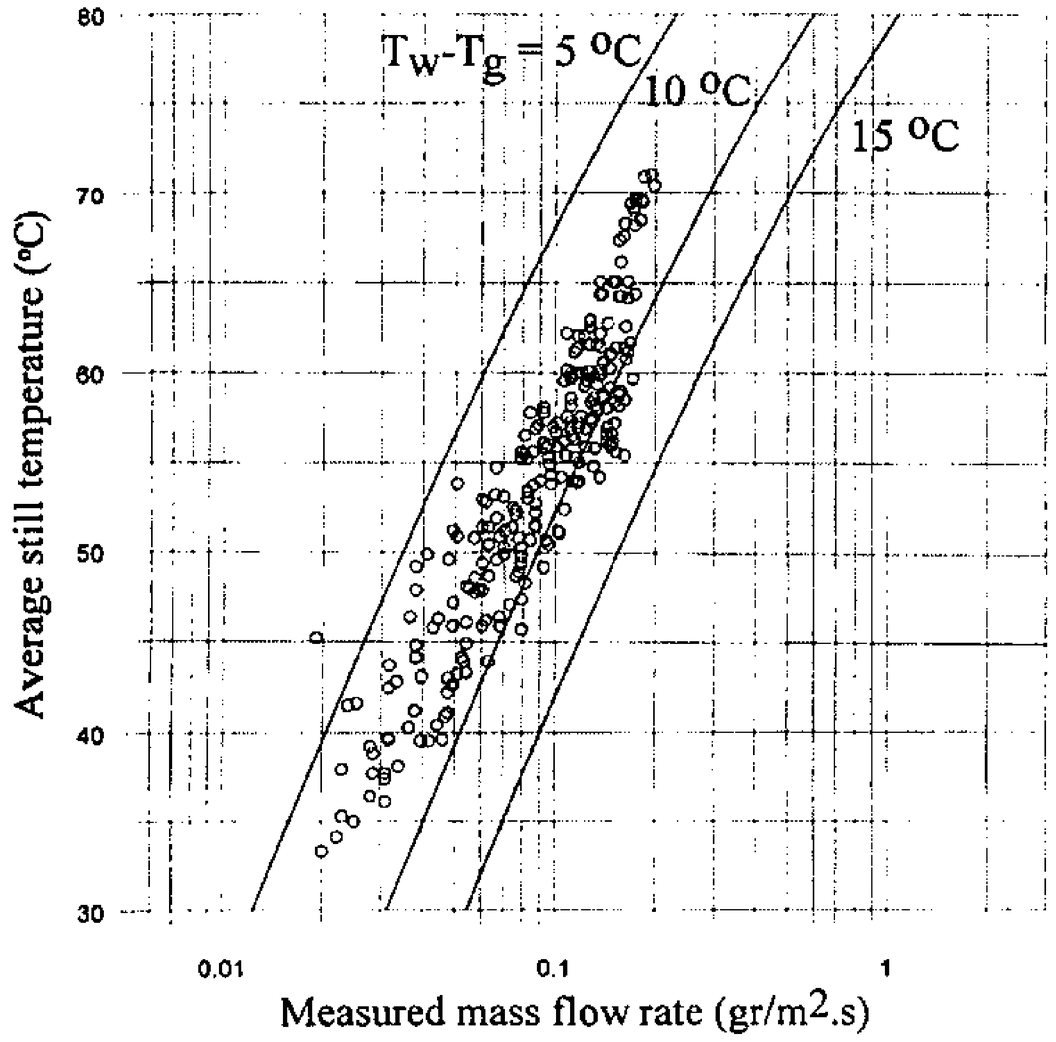

Fig. 6. The dependence of the average still temperature on mass outflow of yield for the three fixed values $\Delta T = T_w - T_g$ of 5, 10 and 15 °C according to predictions from the theoretical model. All derived measurements were comparatively plotted with uniform data points in the same figure.

about 20% of the sample belongs to the temperature difference range of $10 < \Delta T < 15$ °C. As regards the average temperature level, it was found that about 62% of the whole sample of derived data belongs to the average temperature range between $30 < \overline{T} < 60$ °C, while about 38% is distributed within the $72 > \overline{T} > 60$ °C region, something which classifies the entire set of data as medium to high temperature measurements.

As derived from the fundamental theory, the crucial parameters affecting the performance and yield outflow are the temperature difference ΔT and the average operational temperature of the system. Aiming at evaluating their influence on mass outflow for the entire range of practical average temperatures and typical fixed temperature differences of $\Delta T = 5$, 10 and 15 °C, the temperatures t_w and t_g were calculated by the expressions, $t_w = \overline{t} + \Delta T/2$ and $t_g = \overline{t} - \Delta T/2$. These were employed for the evaluation of the corresponding convective heat transfer coefficient and yield according to expressions (5) and (8) respectively. The results which have been plotted in Fig. 6 show the dependence of the average still temperature on mass outflow for the three fixed values $\Delta T = T_w - T_g$ of 5, 10 and 15 °C corresponding to the three plotted solid lines. It is worth noting from this plot that a ΔT increase from 5 to 10 °C and from 10 to 15 °C leads to a corresponding increase of yield by a factor of about 2.6 and 1.7 respectively, almost irrespectively of the average temperature level. At the same time for a fixed typical $\Delta T = 10$ °C an increase of average temperature by 20 °C leads to an yield increase by a factor of about 3.2 which slightly increases with average still temperature.

In the same plot the complete set of measured data corresponding to all runs were also plotted with uniform data points which are spread in the average temperature range between about 33 and 72 °C. The proper distribution of data points between the theoretical constant ΔT lines of 5–15 °C, and more specifically their higher density between $\Delta T = 5$ and 10 °C, which becomes even more pronounced at slightly lower than $\Delta T = 10$ °C, confirms the validity of the theoretical model to predict measurements at least as far as the derived measurements is concerned.

5. Conclusions

The aim of the present investigation was to exploit the derived results comprising a substantial body of field experimental measurements in passive solar stills, in order to acquire an improved level of confidence and verify the validity of an alternative mass transport theoretical model based on the Chilton–Colburn analogy approach.

Extensive calculations taking into consideration constant and temperature depended thermophysical properties for the evaluation of the convective heat transfer coefficient based on the application of the Chilton–Colburn mass transfer model, has allowed the presentation of direct comparisons between theoretical results and measurements. It was derived that the model is suitable for fairly accurate predictions of mass transfer, at least as far as the investigated broad range of the derived measurements is concerned. According to the present investigation, it is derived that although the prediction accuracy is very good even when using the simplified convective heat transfer coefficient model based on the fixed thermophysical properties assumption, the consideration of the temperature depended thermophysical property assumption leads at an even more precise prediction of measurements, especially at higher operating temperatures. Although these measurements have been carried out in a carefully thermally insulated experimental device in a typical sunny Mediterranean climate during mid summer, they covered operational conditions up to average temperatures slightly higher than 72 °C, which is believed to be the typical maximum temperature corresponding to the summer field operation of ordinary design solar stills under sunny, hot and dry Mediterranean climate. It is believed that this model may become a valuable research tool, suitable for application at a wide range of operating conditions, although additional validating investigations would be required toward this aim. These should refer to even higher average temperatures, which however are certainly not easy to develop in the field, unless additional energy input could become

available, to allow close to normal boiling point temperature measurements.

Nomenclature

A_0 to A_4	Numerical constants
c_p	Specific heat capacity (J/kg K)
B_0 to B_3	Numerical constants
C_0 to C_4	Numerical constants
D	Diffusion coefficient (m^2/s)
F_0 to F_4	Numerical constants
g	Acceleration of gravity (m/s^2)
Gr	Grashof dimensionless number,$Gr = g\cdot\beta\cdot\Delta T\cdot L^3/\nu^2$
h	Heat or mass transfer coefficient (w/m^2 K)
k	Thermal conductivity (w/m K)
K_0 to K_3	Numerical constants
L	Characteristic length (m)
Le	Lewis dimensionless number,$Le = \alpha/D$
$\dot{m}$	Per unit still area mass flow rate (kg/m^2 s)
M	Molar mass (kg/kmol)
N_0 to N_4	Numerical constants
Nu	Nusselt dimensionless number
P	Pressure (kPa)
Pr	Prandtl dimensionless number,$Pr = \nu/\alpha$
Q_0 to Q_2	Numerical constants
R	Gas constant (kJ/kg K)
Ra	Rayleigh dimensionless number,$Ra = g\cdot\beta\cdot\Delta T\cdot L^3/\nu\cdot\alpha$
Ra^*	Modified dimensionless Rayleigh number,$Ra^* = g\cdot\beta\cdot\Delta T^*\cdot L^3/\nu\cdot\alpha$
Sc	Schmidt dimensionless number,$Sc = \nu/D$
St	Stanton dimensionless number, $St = h_{cv}/\rho\cdot V\cdot c_p$
St_{ms}	Mass Stanton dimensionless number,$St_{ms} = h_{ms}/V$
t	Temperature (°C)
T	Absolute temperature (K)
$\bar{t}$	Average temperature, (°C),$\bar{t} = t_w + t_g/2$
ΔT	Temperature difference (°C or K),$\Delta T = T_w - T_g = t_w - t_g$
ΔT^*	Equivalent temperature difference (°C or K)

Greek letters

α	Thermal diffusivity (m^2/s)
β	Coefficient of volumetric thermal expansion (K^{-1})
Δ	Difference
λ_1 to λ_2	Numerical constants
μ	Viscosity (kg/m s)
ξ_1 to ξ_2	Numerical constants
ρ	Density (kg/m^3)

Subscripts

a	Air
cv	Convective
ms	Mass
g	Glazing
LM	Logarithmic mean
m	Mixture, average
me	Measured
o	Total, barometric
p	Predicted
w	Water, brine, water vapor

References

[1] G.A.G. Lof, Solar distillation, in: K.S. Springler, H.D.K. Laird (Eds.), Principles of Desalination, second ed., Academic Press, N.Y., London, San Fransisco, 1980, pp. 679–721 (Chapter 11), Part B.

[2] R.V. Dunkle, Solar Water Distillation: The Roof TypeStill and a Multiple Effect Diffusion Still. ASME Proc. Int. Heat Transfer Conf. Part V, Int. Develop. Heat Transfer, Univ. of Colorado, Boulder Colo, 1961.

[3] J.A. Clark, The steady-state performance of a solar still, Solar Energy 44 (1) (1990) 43–49.

[4] A.K. Tiwari, G.N. Tiwari, Effect of water depthson heat and mass transfer in a passive solar srtill: in summer climatic condition, Desalination 195 (2006) 78–94.

[5] V.K. Dwivedi, G.N. Tiwari, Comparison of internal heat transfer coefficients in passive solar stills by different thermal models: an experimental validation, Desalination 246 (2009) 304–318.

[6] P.T. Tsilingiris, Analysis of the heat and mass processes in solar stills – the validation of a model, Solar Energy 83 (2009) 420–431.

[7] P.T. Tsilingiris, Modelling heat and mass transport phenomena at higher temperatures in solar distillation systems – the Chilton-Colburn analogy, Solar Energy 84 (2010) 308–317.

[8] M.A.S. Malik, G.N. Tiwari, A. Kumar, M.S. Sodha, Solar Distillation, Pergamon Press, Oxford, N.Y., 1982.

[9] R.S. Adhikari, A. Kumar, A. Kumar, Estimation of mass-transfer rates in solar stills, Int. J. Energy Res. 14 (1990) 737–744.

[10] M.A.A. Porta-Gandara, E.A. Rubio, J.L.A. Fernandez, Experimental measurement of the water to cover heat transfer coefficient inside shallow solar stills, Appl. Therm. Eng. 18 (1998) 69–72.

[11] E. Rubio, M.A. Porta, J.L. Fernandez, Cavity geometry influence on mass flow rate for single and double slope solar stills, Appl. Therm. Eng. 20 (2000) 1105–1111.

[12] G.N. Tiwari, R. Tripathy, Study of heat and mass transfer in indoor conditions for distillation, Desalination 154 (2003) 161–169.

[13] S. Kumar, G.N. Tiwari, Estimation of convective mass transfer in solar distillation systems, Solar Energy 57 (6) (1996) 459–464.

[14] B. Djebedjian, M.A. Rayan, Theoretical investigation on the performance prediction of solar still, Desalination 128 (2000) 139–145.

[15] M. Jakob, Heat Transfer, first ed., vol. 1, Wiley, NY, 1949.

[16] W.H. McAdams, Heat Transmission, third ed., Mc Graw-Hill, 1958.

[17] K.G.T. Hollands, G.T. Raithby, L. Konicek, Correlation equations for free convection heat transfer in horizontal layers of air and water, Int. J. Heat Mass Transfer vol. 18 (1975) 879–884.

[18] K.G.T. Hollands, Multi-Prandtl number correllation equations for natural convection in layers and enclosures, Int. J. Heat Mass Transfer 27 (3) (1984) 466–468.

[19] V.A. Baum, R. Bairamov, Heat and mass transfer processes in solar stills of hotbox type, Solar Energy 8 (1963) 78–82.

[20] B.F. Sharpley, L.M.K. Boetler, Evaporation of water into quiet air, Ind. Eng. Chem. 30 (1938) 1125–1131.

[21] P.T. Tsilingiris, The influence of binary mixture thermophysical properties in the analysis of heat and mass transfer processes in solar distillation systems, Solar Energy 81 (2007) 1482–1491.

[22] P.T. Tsilingiris, Thermophysical and transport properties of humid air at temperature range between 0 and 100 C, Energy Convers. Manag. 49 (2008) 1098–1110.

[23] Ahmad Taleb Shawaqfeh, Mohhamed Mehdi Farid, New development in the theory of heat and mass transfer in solar stills, Solar Energy 55 (6) (1995) 527–535.

[24] Zheng Hongfei, Zhang Xiaoyan, Zhang Jing, Wu Yuyuan, A group of improved heat and mass transfer correllations in solar stills, Energy Convers. Manag. 43 (2002) 2469–2478.

[25] J.M. Coulson, J.F. Richardson, Chemical Engineering, fifth ed., vol. 1, Butterworth Heineman, 1997.

[26] T.H. Chilton, A.P. Colburn, Mass transfer (absorption)coefficients-prediction from data on heat transfer and fluid friction, Ind. Eng. Chem. 26 (1934) 1183.

[27] P.T. Tsilingiris, Prediction and measurement of mass transport in experimental solar stills, Solar Energy 85 (2011) 2561–2570.